Ultrasonics Sonochemistry 92 (2023) 106229

Contents lists available at ScienceDirect

Ultrasonics Sonochemistry

journal homepage: www.elsevier.com/locate/ultson

Inhibitory effects of ultrasonic and rosmarinic acid on lipid oxidation and lipoxygenase in large yellow croaker during cold storage

Ting-ting Chai, Yang-na Huang, Shao-tian Ren, Dan-li Jin, Jing-jing Fu, Jun-yan Guo, Yue-wen Chen *

School of Food Science and Biotechnology, Zhejiang Gongshang University, Hangzhou, Zhejiang 310035, China
Zhejiang Provincial Collaborative Innovation Center of Food Safety and Nutrition, Zhejiang Gongshang University, Hangzhou, Zhejiang 310035, China

ARTICLE INFO

Keywords:
Ultrasound
Rosmarinic acid
Lipid oxidation
Lipoxygenase
Multi spectroscopy
Molecular docking

ABSTRACT

Lipid oxidation will lead to the deterioration of flavor, color and texture of aquatic products with high fatty acid content. The mechanism of ultrasound (US) combined with rosmarinic acid (RA) on lipid oxidation and endogenous enzyme activities of large yellow croaker during cold-storage (4 ℃) was investigated. The result showed that the US and RA have synergistic effects in delaying lipid oxidation and inhibiting endogenous lipase and lipoxygenase (LOX) activities related to oxidation. The inhibition of LOX activity by RA was dose-dependent, and US showed a negative effect on the inhibition of enzyme activity in the presence of low concentration RA. Moreover, RA changes the enzyme structure through static fluorescence quenching and interaction with enzyme molecules. Hydrogen bonding and hydrophobic interaction are the main interaction forces between RA and LOX. This study could provide basic mechanism of US treatment cooperating with polyphenols to inhibit lipid oxidation during food preservation.

1. Introduction

Fresh large yellow croaker is rich in nutrients such as protein and lipids. It is considered to be one of the most economically valuable fish in China [1]. However, it susceptible to lipid oxidation and bad odor due to the action of microorganisms and endogenous enzymes during storage and transportation [2]. Previous study indicated that the oxidation products of lipids can accelerate the oxidation of proteins, which leads to deterioration of some functional characteristics of proteins, such as decreased water holding capacity and reduced solubility, thus affecting the shelf life of fish [3]. Therefore, it is necessary to develop a new anti-oxidation and fresh-keeping measure to inhibit lipid oxidation and maintain the quality of large yellow croaker samples.

Recently, the natural antioxidants such as flavonoids and polyphenols extracted from plants have been widely used to extend the shelf life of aquatic products during storage and circulation [4,5]. Rosmarinic acid (RA) is a phenolic acid derivative natural antioxidant existing in Labiatae plants [6]. Previous study indicated that RA can block the chain reaction of lipid oxidation by chelating metal ions and scavenging free radicals, and thereby slowing down lipid oxidation in aquatic products and meat [7]. In addition, it was also found that RA can effectively inhibit the growth of common contaminating bacteria and delay product corruption [4]. Li, Liu, Shen, Mei and Xie [8] shown that RA as a natural antioxidant plays a crucial role in the storage and preservation of fresh half-smooth tongue sole fillets.

Ultrasound (US) is a promising new technology, which has been widely used in food sterilization, tenderization, pickling and extraction [9]. The cavitation effect and physical mass transfer effect produced by US can be used to change the characteristics of food, shorten the processing time, and have the advantages of safety, efficiency and green [9,10]. In addition, US can inhibit the activity of certain enzymes and the growth of microorganisms in food [9,11]. In order to effectively control microbial spoilage and oxidation of aquatic products during storage, the combined effect of US and polyphenols were considered. Sae-leaw, Benjakul, and Vongkamjan [12] found that US may enhance the migration of Epigallocatechin gallat (EGCG) solution into shrimp, thus delaying the blackening disease and quality deterioration of pre-cooked Pacific white shrimp during cold storage. Liu, Li, Wu, Yang, Zhou and Zhu [10] indicated that the combined treatment of US and bamboo leaf antioxidant can availably delay the protein and lipid oxidation of

* Corresponding author at: School of Food Science and Biotechnology, Zhejiang Gongshang University, Xiasha University Town, Xuezheng Str. 18, Hangzhou 310018, China.
E-mail address: chenyw@zjgsu.edu.cn (Y.-w. Chen).

https://doi.org/10.1016/j.ultsonch.2022.106229
Received 11 October 2022; Received in revised form 10 November 2022; Accepted 18 November 2022
Available online 19 November 2022

scallop during cold storage. However, the mechanism of the combined effects of US and phenolic acids on lipid oxidation and endogenous enzyme activity during fish cold storage still unclear.

Thus, the main purpose of this study is to evaluate the changes of lipid oxidation and its effects on related enzyme activities of large yellow croaker during cold storage after US and RA treatment. Meanwhile, the interaction mode and inhibition mechanism of US and RA on the endogenous lipoxygenase (LOX) of large yellow croaker were analyzed by in vitro enzyme activity inhibition kinetics, multi spectroscopy and molecular docking methods. This study provides a theoretical basis for the application of US and RA in the anti-oxidation and fresh-keeping of aquatic products.

2. Material and methods

2.1. Chemical

RA (90 %, HPLC) was bought from Yuanye Biotechnology Co., Ltd. (Shanghai, China), p-nitrophenyl palmitate (4-NPB) was purchased from Aladdin Biochemical Technology Co., Ltd. (Shanghai, China), p-nitrophenol, L-ascorbic acid, petroleum ether, isooctane, isopropanol, disodium hydrogen phosphate dodechydrate, sodium phosphate dihydrate, ethylenediaminetetraacetic acid (EDTA), trichloroacetic acid Linoleic acid were purchased from Macklin biochemical Co., Ltd. (Shanghai, China), and all chemicals were of analytical grade.

2.2. Methods

2.2.1. Fish sample preparation

The large yellow croaker was transported to the laboratory in ice bath from Dachen Huangdao fenced breeding base (Taizhou, China) within 2 h and stored at −60 °C. The large yellow croaker was cut into fish pieces (35 ± 5 g), washed with sterile water for three times, and then the fish meat was divided into four groups. After that, the fish meat was soaked in different solutions at the ratio of 1:2 (m/v) for 10 min at 4–10 °C: C (original sample as negative control); VC (treated with 0.05 % L-ascorbic acid solution as a positive control); R (0.05 % RA solution); RU (0.05 % RA solution impregnated with ultrasonic treatment at 30 kHz and 400 W (DL-820E, Shanghai Zhixin Instrument Co., ltd., China). Then, they were separately packed in polyethylene composite bags (20 wires thick, 100 ℃ high temperature resistant) and vacuumized at − 0.02 MPa (P290, Shineye Inc., China). All samples were stored at 4 °C for refrigeration and measured every 2 days.

2.3. Determination of lipid oxidation stability

2.3.1. Peroxide value (POV)

The determination of POV refers to the method of Yuan, Chen, Cai, Dong, Wang and Zheng [13]. Dissolve the lipids extracted from fish meat with chloroform glacial acetic acid mixture, add saturated potassium iodide for reaction, titrate with sodium thiosulfate standard solution (0.002 M) until the solution is light yellow, then add starch indicator, and continue to drip sodium thiosulfate solution until the solution is blue. The determination result is expressed by the mass fraction of peroxide and iodine.

2.3.2. Thiobarbituric acid reactive substance (TBARS)

TBARS was determined by referring to the method of Chen, Cai, Shi, Dong, Bai, Shen, Jiao, Zhang and Zhu [14]. 5 g fish meat was weighed and 25 mL of trichloroacetic acid solution (7.5 %, v/v) was added to the beater (4192 handheld electric mixer, Braun Inc., Germany) for homogenization for 30 s, filter the homogenized solution with filter paper and collect the filtrate. Add thiobarbituric acid (TBA, 0.02 M) of the same volume as the filtrate, heat it in the boiling water bath in the glass tube for 40 min. Then add chloroform of the same volume as the filter material after cooling and let it stand for stratification after vortex shaking. Finally measure the absorbance value of the supernatant at 532 nm and 600 nm (UV–visible Spectrophotometer Model 2100, Unico, China) respectively. The result is expressed by the mass (mg) of malondialdehyde (MDA) contained in each kilogram of meat sample.

2.4. Extraction and activity determination of endogenous enzymes

The extraction of crude lipase and LOX solution and determination of enzyme activity were carried out according to the method of Cao, Huang, Zhu, Song, Xiong, Manyande and Du [15] with slight changes. Briefly, lipase and LOX were extracted by mixing fish muscle samples with Tris-HCl buffer (25 mM, 150 mM NaCl, pH 8.0), phosphate buffer (PBS) (50 mM, 1 mM dithiothreitol, 1 mM EDTA, pH 7.4) at a ratio of 1:5 (w/v), respectively, then homogenized at 4000 rpm at ice bath using a handheld electric mixer. The mixture was stirred in an ice bath for half an hour and centrifuged at 4 °C (10,000×*g*, 20 min). Filter the supernatant with filter paper to obtain crude enzyme solution.

The lipase activity was measured by the 4-NPB method. The 4-NPB was dissolved in isopropanol to prepared substrate solution. The diluted lipase (800 μL) and Tris-HCl buffer (2 mL) was mixed and then the substrate solution (400 μL) was added. Use ultraviolet visible spectrophotometer to measure the absorbance at 410 nm and the enzyme activity unit was defined as the enzyme released per μmol of p-nitrophenol in 1 min.

To obtain LOX activity, the linoleic acid was dissolved in distilled water containing Tween 20 to prepare LOX substrate solution and adjust the pH to 9.0 with NaOH. Diluted LOX solution (200 μL) was mixed with citric acid buffer (50 mM, 2.4 mL, pH 5.5) and incubated at room temperature for 10 min. Then add the substrate solution (200 μL) to start the reaction and record the absorbance at 234 nm. One unit of LOX activity was defined as an increase of 0.001 absorbance per minute.

2.5. Determination of inhibition mechanism of enzyme activity in vitro

2.5.1. Extraction and purification of LOX

The preparation of LOX crude enzyme solution is the same as that in section 2.4., Mix the obtained supernatant of crude enzyme with 40 % and 20 % ammonium sulfate by weight in turn, stirred it in ice bath for half an hour and centrifuge it at 4 °C (10,000×*g*, 10 min). Finally, collect LOX precipitate into dialysis bag and desalted with the previous PBS for 24 h, with buffer changes every 6 h.

2.5.2. SDS-Page

According to the method of Sheng, Su, Han, Chen, Cao, Zhang, Jin and Ma [16], 12 % of the separated gel and 4 % of the stacked gel were used for SDS-PAGE. The samples were diluted by PBS to make the concentration of protein of 0.5 mg/mL. 20 μL of the sample was loaded onto the electrophoresis gel and the standard protein was used as a marker (10–250 kDa) at 110 V (DYY-6D, Beijing Liuyi Biotechnology Co., Ltd., China). Finally, the gel was stained and decolored to show the protein band.

2.5.3. Enzyme inhibition test

The determination of LOX activity is the same as section 2.4, in which 200 uL RA solution is added to the mixed solution. The inhibition rate was determined by setting the concentration of LOX and linoleic acid to 0.2 mg/mL and 50 Mm, respectively. Two groups of samples were prepared at the same time. One group was incubated with the mixed solution at 25 °C for 10 min under 400 W US (Group U) and the other group was incubated at 25 °C for 10 min (Group C). Set the following concentrations for the inhibition type experiment: LOX: 0.05, 0.1, 0.2, 0.3, 0.4 mg/mL; RA: 0, 0.1, 0.2 mg/mL; Linoleic acid: 50 mM. Set the following concentrations for the inhibition kinetics experiment: LOX: 0.2 mg/mL; RA: 0, 0.1, 0.2 mg/mL; Linoleic acid: 3.125, 6.25, 12.5, 25, 50 mM (Table 1).

Table 1
Quenching constants (K_{SV}), binding constants (K_b) and thermodynamic parameters of RA-LOX under different temperatures.

Sample	Temperature (K)	K_{sv} (10^4 L/mol)	K_q (10^{12} L/mol·s)	K_b (10^5 L/mol)	n	ΔG (kJ/mol)	ΔH (kJ/mol)	ΔS (J/mol·K)
LOX	298	3.40	3.40	3.07	1.10	−2.78	−29.77	−81.51
	304	2.88	2.88	2.75	1.23	−2.56		
	310	1.87	1.88	2.19	1.23	−2.02		

K_{sv}, the quenching constant; K_q, biomolecular quenching constant; K_b, binding constant; ΔH, enthalpy change; ΔS: entropy change; ΔG, Gibbs free energy change.

2.5.4. Fluorescence spectra measurement

The interaction of LOX solution and different concentrations of RA solution at 298 K, 303 K and 310 K was studied with reference to the method of Fu, Sun, Tan, Zhang, Chen and Song [17] with slight changes. Specifically, the final concentration of RA was 0, 0.05, 0.1, 0.2, 0.4, 0.8×10^{-4} M respectively by continuously titrating RA into 3 mL enzyme solution (0.2 mg/mL). One group was sonicated for 10 min (Group U), and the other group was not treated (Group C). Measuring the fluorescence spectrum of the solution with the RF- 6000 spectrometer (Shimadzu, Kyoto, Japan), the excitation wavelength is set at 280 nm and the emission scanning range is 290–450 nm. The synchronous fluorescence was determined according to the method of Zhu, Sun, Wang, Xu, & Wang [18]. The quenching constant was obtained by calculating the fluorescence intensity at the peak, and the Stern-Volmer equation Eq (1) was used to evaluate the quenching of LOX fluorescence by RA [19].

$$\frac{F_0}{F} = 1 + K_{sv}[Q] = 1 + K_q\tau_0\,[Q] \tag{1}$$

where, F and F_0 represent the fluorescence intensity of LOX in the presence and absence of RA, respectively, [Q] represents the concentration of RA, K_q means the bimolecular quenching rate constant, K_{sv} means the quenching constant, and τ_0 (10^{-8} s) means the average lifetime of the protein without quencher.

The binding constant (K_b) and the number of binding sites (n) of LOX can be obtained according to Eq. (2) [20].

$$\log\left(\frac{F_0\text{-}F}{F}\right) = \log K_b + n \log [Q] \tag{2}$$

The fluorescence spectrum were also used to determine the thermodynamic parameters of binding, including entropy change (ΔS), enthalpy change (ΔH) and Gibbs free energy change (ΔG), based on Eqs. (3) and (4) [21].

$$\log K_b = -\frac{\Delta H}{2.303RT} + \frac{\Delta S}{2.303R} \tag{3}$$

$$\Delta G = \Delta H - T\Delta S = -RT \log K_b \tag{4}$$

where T is absolute temperature (K) and R is the universal gas constant [8.314 J/(mol·K)].

2.5.5. UV–visible (UV–vis) spectroscopy measurement

According to the method of Xu, Cao, Manyande, Xiong and Du [19], the absorption spectrum of the sample in the range of 200–450 nm was measured using a spectrophotometer (UV-2600, Shimadzu, Inc., China). The preparation of sample solution is the same as section 2.5.4.

2.5.6. Fourier transform infrared spectroscopy (FT-IR)

The determination of FT-IR refers to the method proposed by Shen, Bu, Yu, Chen, Liu, Ding and Mao [22]. The sample solution was prepared in the same way as in section 2.5.4 and lyophilized, Then the freeze-dried sample powder was mixed with KBr and pressed into pieces, with KBr without sample as the background spectrum. After that, the spectrum was determined under the parameters of 4000–400 cm^{-1} spectral scanning, 4 cm^{-1} resolution and 32 scanning times (NICOLET IS5, Thermo Scientific, Germany).

2.5.7. Molecular docking

Docking simulation technology is a convenient and effective means to explore the interaction between small molecules and target targets [22,23]. The AutoDock Vina (http://vina.scripps.edu/) was used for docking research of small molecules RA and LOX. The protein crystal structure LOX (PDB ID:2P0M) used for docking was passed through the RCSB database (https://www.rcsb.org/) Obtain; The 3D structure of small molecule RA (PubChem CID:5281792) was acquired from the PubChem database(https://pubchem.ncbi.nlm.nih.gov/). Before the start of docking, both ligands and receptors were pretreated with dehydration and hydrogenation, and AVOGADR software was used to minimize their energy under the MMFF94 force field. SMINA was used for docking. PyMOL (https://www.pymol.org) was used visual analysis of docking results.

2.6. Statistical analysis

Samples of fish pieces were analyzed in triplicate and data were expressed as means ± SD. The differences between the treatment groups were measured by Duncan's test in SPSS and statistical significance was set at $P < 0.05$.

3. Results and discussion

3.1. Determination of lipid oxidation

POV is mainly used to determine the content of hydroperoxide in food [13]. As shown in Fig. 1A, the POV of each group appeared a trend of rising at first and then reducing. This may be due to the POV accumulated at the beginning of storage. However, with the extension of storage time, the decomposition rate of peroxide generated by oxidation was greater than its generation rate, and POV gradually decreased. The RU treatment groups obtained the lowest POV of all groups during 8 d storage. This may be due to the RU treatment of cold-storage fish can inhibit their lipid oxidation. This result is consistent with Liu, Li, Wu, Yang, Zhou and Zhu [10], who indicated that the RU treatment could effectively retard lipid oxidation.

The level of TBARS value reflects the amount of secondary oxidation products of lipids [14]. The TBARS value of all groups ranged from 0.53 to 1.50 (Fig. 1B). The RA treatment showed a better capacity to restrain the increase of TBARS value than VC groups. This may be because RA can directly remove oxygen free radicals in food [24]. Jongberg, Torngren, Gunvig, Skibsted and Lund [24] also found that green tea and rosemary extract can significantly improve the antioxidant performance of samples and prevent the production of TBARS. Moreover, the RU treatment group exhibited lower TBARS value than RA treatment group. This result indicated that RU treatment can better inhibit lipid oxidation of large yellow croaker during cold-storage.

3.2. Changes in lipase and LOX activities in large yellow croaker meat

Lipase and LOX are two endogenous enzymes closely related to lipid oxidation [15]. The changes of endogenous enzyme activities during storage of fish meat samples after different treatments are shown in Fig. 1E-F. The lipase activities of all samples increased rapidly in the first 4 d ($P < 0.05$) and then decreased (Fig. 1E). This is consistent with the

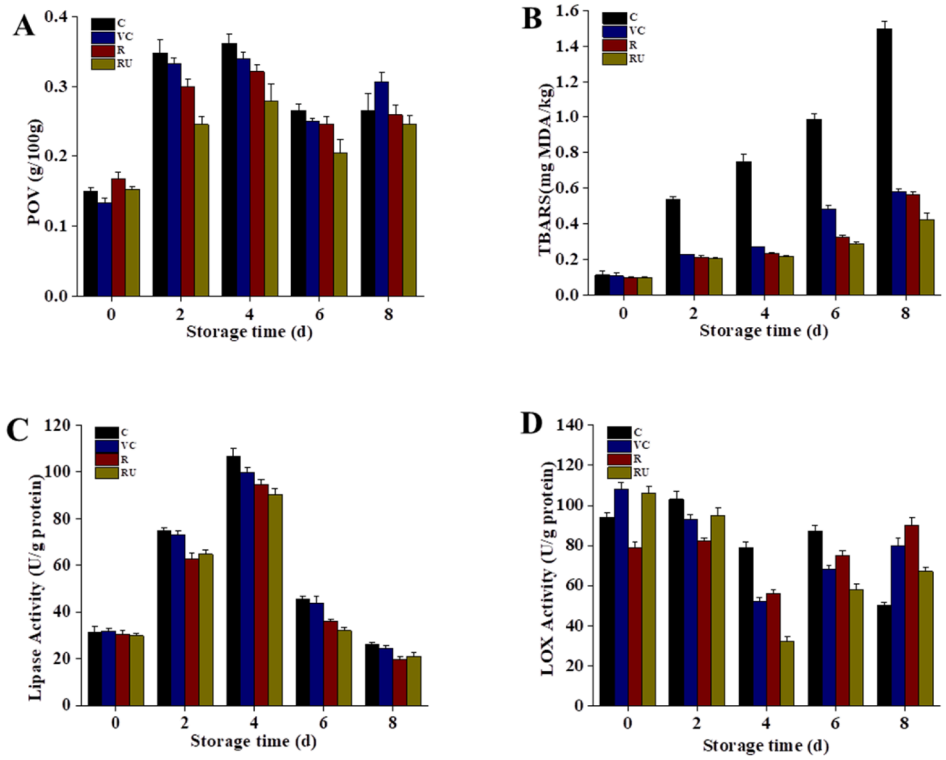

Fig. 1. Changes of TBARS value (A), POV (B), lipase activity (C) and LOX activity (D) of large yellow croaker during storage. Note: C: Raw samples as control; VC: Immersion in 0.05 % VC solution for 10 min; R: Immersion in 0.05 % RA solution for 10 min; RU: Immerse 0.05 % RA solution with ultrasonic treatment for 10 min at 30 KHz and 400 W.

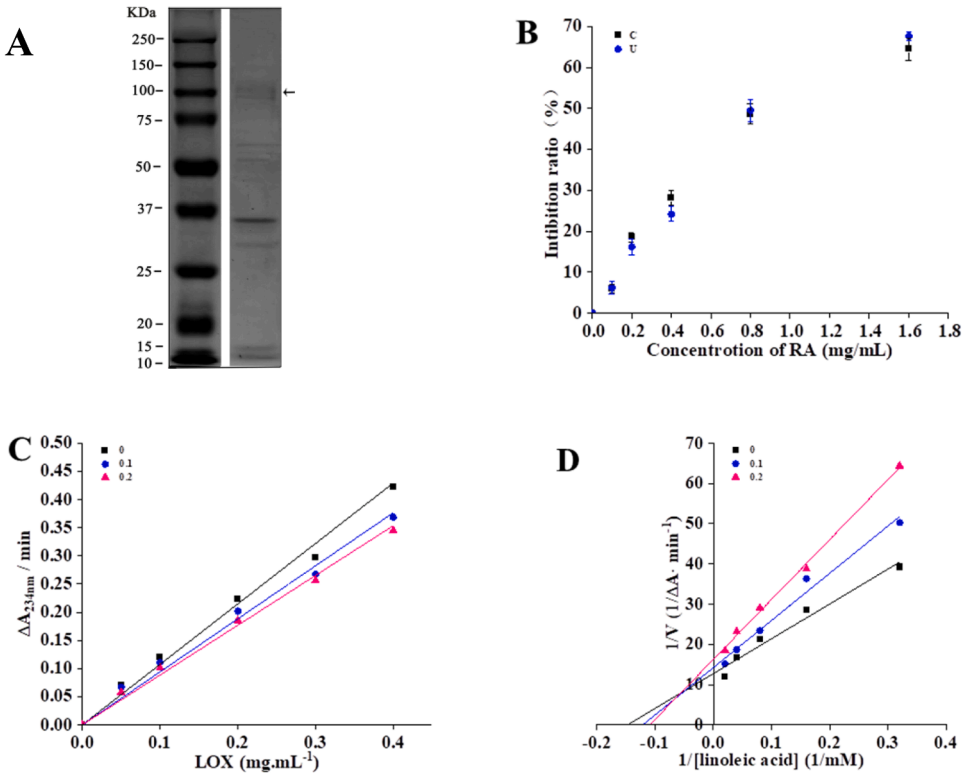

Fig. 2. Results of purity (SDS-PAGE) and inhibitory activities of LOX. Note: A: Left-Markers; Right-LOX; B: Inhibitory ratios of LOX (c_{LOX} = 0.2 mg/mL; $c_{linoleic\ acid}$ = 50.0 mM); C: Inhibitory types of LOX ($c_{linoleic\ acid}$ = 50.0 mM; c_{RA} = 0.0–0.2 mg/mL); D: Inhibitory kinetics of LOX (c_{LOX} = 0.2 mg/mL; $c_{linoleic\ acid}$ = 3.125–50.0 mM; c_{RA} = 0.0–0.2 mg/mL).

change trend of lipase activity during storage of Grass carp treated with chlorogenic acid [25]. During storage, there was no significant difference between control group (C) and VC on lipase activity ($P > 0.05$). The addition of RA could markedly reduce the lipase activity than control group ($P < 0.05$), indicating that RA could induce the decrease of lipase activity, which may be an important reason for its inhibition of lipid oxidation. Moreover, the US treatment further inhibited lipase activity, which may be due to the mechanical and chemical effects of ultrasonic cavitation treatment that change the structure of the enzyme and led to the changes in its activity [11]. After 4 d of storage, LOX activity decreased significantly ($P < 0.05$) and gradually increased in the late stage of storage (Fig. 1F), which is consistent with the change trend of POV. Previous study indicated that the LOX mainly catalyzes unsaturated fatty acids to form unstable hydroperoxides [26]. In addition, the LOX activity in RU group decreased by 69.81 % on the 4th d, which was consistent with the result that RU treatment could inhibit lipase activity.

3.3. Inhibition activity and inhibition kinetics of endogenous enzymes

The inhibition of LOX activity after treatment with different concentrations of RA and combined with US is shown in Fig. 2A. With the increase of RA concentration, the inhibitory rate of RA on LOX activity gradually increased. After RA combined with US treatment, US treatment can promote the improvement of LOX activity in the low concentration range of RA, and the inhibition of LOX activity in the high concentration range of US treatment shows a synergistic effect. This result indicates that US plays a major role when the concentration of RA is low. Dalagnol, Silveira, da Silva, Manfroi, and Rodrigues [27] indicated that the US treatment could modify the enzyme structure of LOX, thereby increasing the activity of it. When the concentration of RA is high, US treatment can accelerate the exposure of hydrophobic groups of LOX, thereby increasing the interaction between LOX molecules and RA, which leads to a decrease in its enzymatic activity [28].

A kinetic diagram of LOX in the presence of different concentrations of RA was constructed to clarify the type of inhibition of RA on LOX. As shown in Fig. 2B, after fitting, each experimental group was a straight line passing through the origin, and the slope decreased with the increase of RA concentration, indicating that the type of inhibition of RA on LOX was reversible inhibition [29]. The inhibition type of LOX was evaluated by plotting the Lineweaver-Burk curve of each group at different RA concentrations (Fig. 2C). The value of K_m (Michaelis-Menten) increased with the rise of RA concentration (from 6.80 mg/mL to 9.15 mg/mL), while the value of V_m (maximum velocity) was opposite (from 0.078/min to 0.061/min), indicating that the inhibition type of LOX by RA was mixed inhibition. The inhibitory effect of chlorogenic acid on LOX extracted from grass carp muscle obtained the similarly result [15].

3.4. SDS-PAGE analysis of LOX

The molecular weight of LOX is found to be about 97 kDa in grass carp and mackerel [15,30]. The molecular weight distribution of LOX extracted from large yellow croaker is shown in Fig. 2A. The 95 kDa band is considered as the target LOX, and other bands may be LOX isomers or their degradation products. LOX less than 90 kDa is found to be inactive in plants [31] (Fig. 3).

3.5. Fluorescence spectrum analysis

The fluorescence spectrum of tryptophan (Trp) with aromatic ring structure in protein is often used as a sensitive index to judge the conformational change of protein [16]. The fluorescence emission spectra of group C and group U were measured at 298 K (Fig. 4A). With the raise of RA concentration, the endogenous fluorescence intensity of LOX gradually weakened and accompanied by the blue shift of the maximum wavelength. This result declares that RA can quench the intrinsic fluorescence of LOX and expose it to a more hydrophobic microenvironment [23,32]. This form of intrinsic fluorescence quenching is related to the interaction between RA and LOX molecules. Compared with group C, the fluorescence intensity of LOX in group U was enhanced after US treatment in the absence of RA, and the fluorescence quenching of LOX was significant in the presence of RA

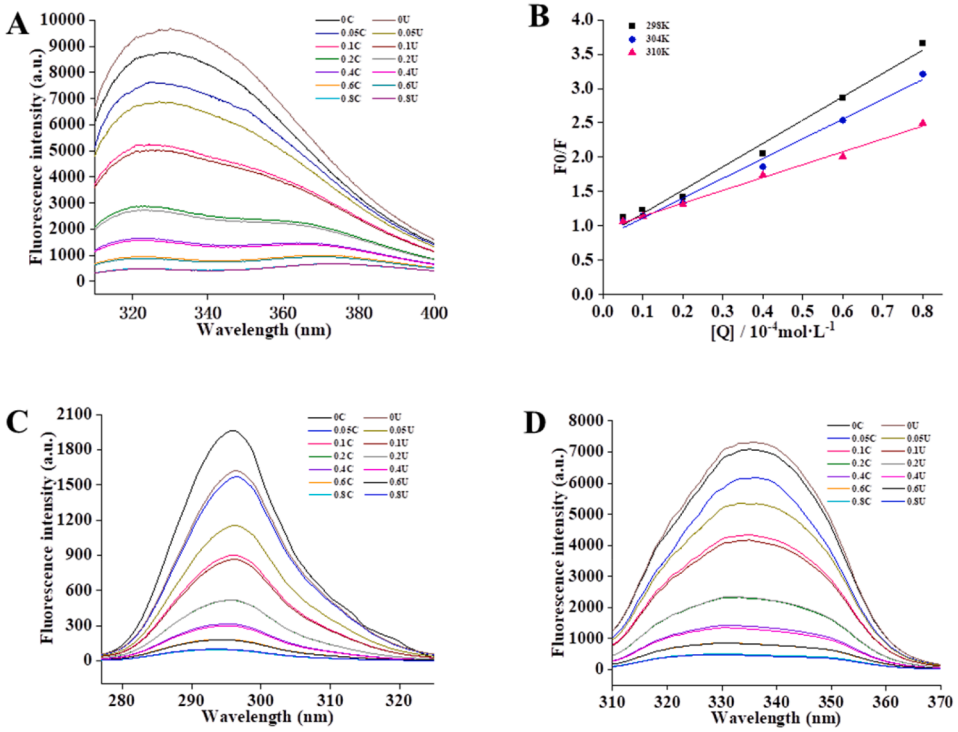

Fig. 3. Fluorescence spectra analysis of the interaction between RA and LOX. Note: c_{RA} = 0.0, 0.05, 0.1, 0.2, 0.4, 0.6, 0.8 × 10^{-4} mol/L; A: Fluorescence spectra (T = 298 K); B: Stern-Volmer plots for fluorescence quenching; C (Δλ = 15 nm) and D (Δλ = 60 nm): Synchronous fluorescence spectrum of LOX.

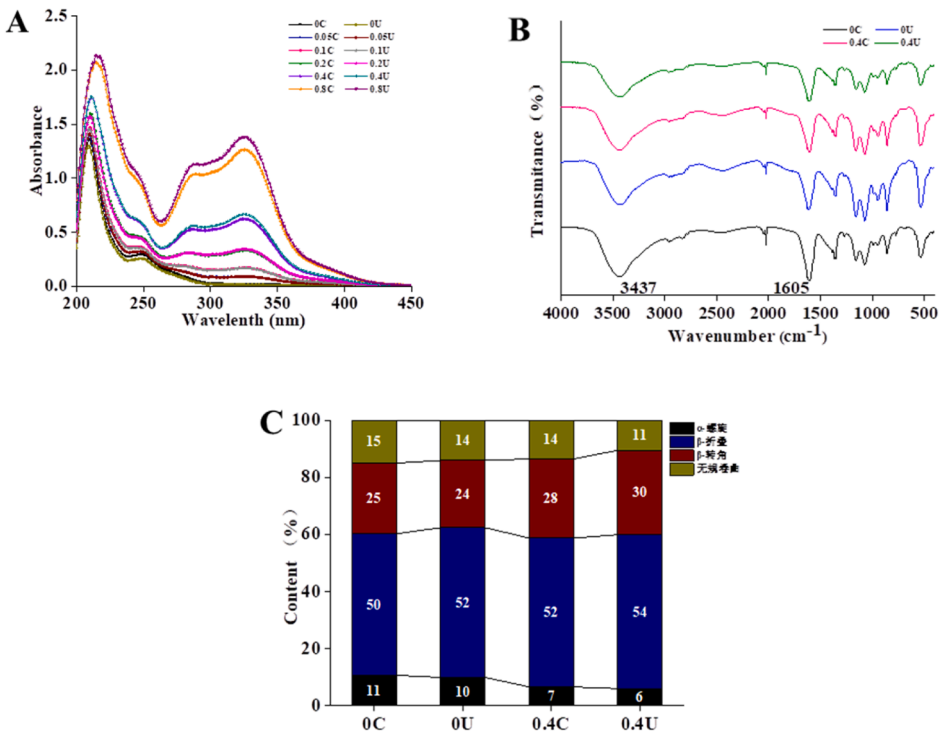

Fig. 4. UV–*vis*/FT-IR spectra of LOX after the interaction of RA. Note: c_{RA} = 0.0–0.8 × 10^{-4} M; A: UV–*vis* absorption; B: FT-IR spectra; C: Conformation changes in secondary structures of LOX.

($P < 0.05$). This may be due to the fact that US promotes the exposure of the internal groups of LOX, such as tryptophan, hydrophobic amino acids and sulfhydryl groups, thus promoting the binding of RA to it [33].

3.5.1. Fluorescence quenching mechanism

The Stern-Volmer curve of the interaction between RA and LOX at different temperatures shows a good linear relationship (Fig. 4B). As shown in Fig. 4E, the quenching constant (K_{SV}) decreases with the promote of temperature, indicating that the complex becomes less stable at higher temperatures [20]. Minimum quenching rate constant (K_q = 1.88 × 10^{12} L·mol^{-1}·s^{-1}) is much higher than the maximum dispersion collision quenching constant (2.00 × 10^{10} L·mol^{-1}·s^{-1}), K_a reduced with the rise of temperature, which shows that the quenching type belongs to static quenching [21]. In addition, the number of binding sites n is around 1, it shows that RA can only have one binding site with LOX and has relatively strong affinity for LOX.

3.5.2. Measurement of thermodynamic parameters

The key thermodynamic parameters for studying the interaction types between phenolic compounds and enzyme proteins are mainly hydrogen bond, van der Waals force, electrostatic interaction and hydrophobic interaction [21,22]. As shown in Fig. 4E, the $\Delta G < 0$ at different temperatures, which indicates that the reaction can proceed spontaneously. The $\Delta H < 0$, indicating that the reaction is exothermic. Moreover, the ΔH, ΔS and ΔG are all negative, which suggests that the complex formed by RA and LOX is mainly maintained by hydrogen bond and van der Waals force [34]. The results of the interaction process are similar to the results of chlorogenic acid inhibiting LOX [15].

3.5.3. Synchronous fluorescence spectrum analysis

When the wavelength between the excitation wavelength and the emission wavelength is Δλ fixed at 15 and 60 nm, the synchronous fluorescence spectrum of the enzyme solution will give the characteristic information of tyrosine (Tyr) and Trp residues respectively [19]. The hydrophilic and hydrophobic changes of the microenvironment where Tyr and Trp residues are located can be used to characterize the effect of RA on the conformation of the enzyme [21,32,34]. With the increase of RA concentration, when Δλ = 15 nm, no significant shift was found in LOX (Fig. 4C), indicating that there was no significant change in the environment near Tyr. When Δλ = 60 nm, the maximum emission wavelength in LOX was slightly blue shifted (Fig. 4D), indicating that the polarity of the microenvironment where Trp is located decreases and the hydrophobicity increases. In addition, the maximum emission wavelength of synchronous fluorescence of group U is lower than that of group C, which reflects the synergistic effect of US and RA on the synchronous fluorescence quenching of LOX. This result is roughly same as that of the previous fluorescence spectral analysis.

3.6. UV–visible spectroscopy analysis

The changes in the UV–*vis* absorption spectra of LOX in the two groups (Group C and group U) were observed after adding different concentrations of RA. As shown in Fig. 5A, with the increase of RA concentration, the absorption peak near 220 nm was enhanced and red shifted, indicating that the skeleton structure of LOX was affected [18]. The raise in absorption intensity and red shift of the peak near 275 nm indicate that a complex is formed between RA and LOX. The absorbance of the complex increases significantly between 250 nm and 350 nm with the increase of RA concentration, and the absorption peak intensity of group U is higher than that of group C. This result indicates that the interaction between RA and LOX is enhanced after RA addition, and US treatment can further enhance this effect. This is the same as the previous fluorescence spectrum results. Moreover, the change of the maximum emission wavelength and the difference of the UV–*vis* absorption spectrum confirm that the quenching mechanism is static quenching again [19].

3.7. FT-IR spectroscopy analysis

The FT-IR spectra of LOX of different treatment groups in the range of 4000–400 cm^{-1} were studied (Fig. 4B). The absorption peak of LOX at 3437 cm^{-1} is caused by the stretching vibration of N—H single bond and

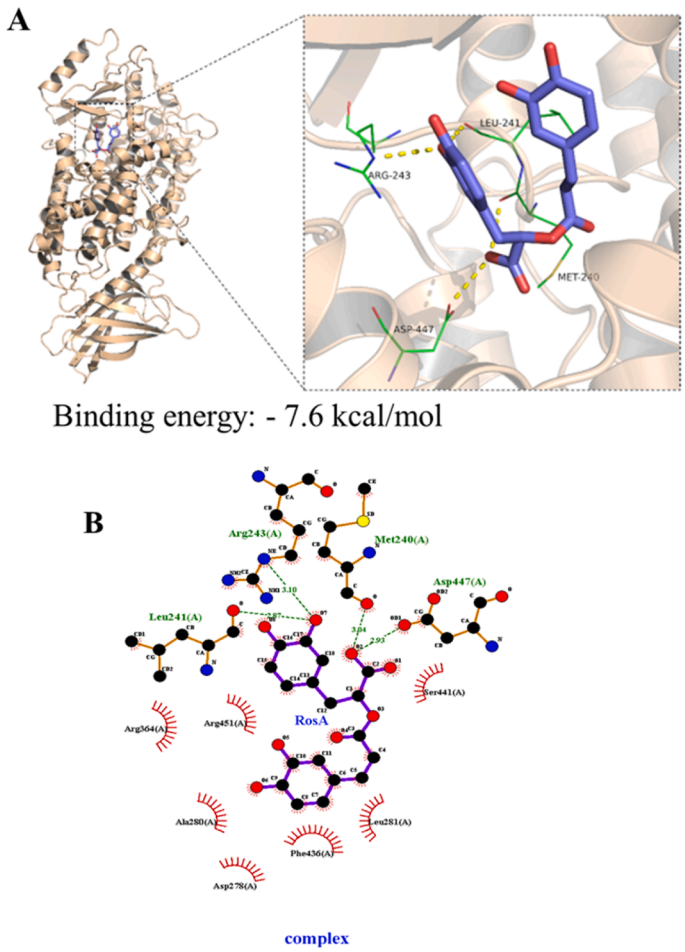

Fig. 5. Molecular docking analysis of the interaction of RA and LOX. Note: A: Results of 3D molecular docking modeling and docking ligand in the binding site; B: Results of 2D molecular docking modeling.

O—H single bond in protein molecules [35]. The peak at 1632 cm^{-1} in the amide I (1700–1600 cm^{-1}) region comes from the stretching vibration of C═O double bond [36]. After treatment with RA and US, the intensity of LOX at the two peaks mentioned above becomes weak, which indicates that RA and US interact with LOX respectively and affect the structure of the enzyme. The secondary structure changes of LOX were further characterized by analyzing the curve fitting spectra within the LOX amide I region [37] (Fig. 4C). Overall, after RA and US treatment, the proportion of α-helix and random coil was dramatically decreased, and the β-sheet and β-turning angle was opposite ($P < 0.05$). Previous studies have shown that the intramolecular hydrogen bonds play an important role in the stability of the α-helical network structure [37,38]. The combination of RA and LOX may weaken the intramolecular hydrogen bonds and strengthen the intermolecular hydrogen bonds, leading to the reduction of the α-helical structure of proteins [35]. Moreover, the US action disrupts the hydrogen bond inside the enzyme protein, exposing the hydrophobic group, thus promoting the unfolding of the α-helical structure of the protein [39,40]. These results and explanations were confirmed by fluorescence analysis and UV results.

3.8. Analysis of molecular docking results

A negative number of binding energies indicate the possibility of binding (Fig. 6C). Generally, a value less than – 5.0 kcal/mol is considered to have a greater possibility of binding. The binding affinity between RA and LOX is – 7.6 kcal/mol, which means that small molecule RA and LOX have ideal potential activity effects. The interaction force between RA and LOX was analyzed using Ligplot software. In the complex LOX-RA, the RA is bound in the LOX protein pocket surrounded by Arg364, Arg451, Ala280, Asp278, Phe436, Leu281, Ser441, Leu241, Arg243, Met240, and Asp447 amino acids. Among them, it forms hydrogen bonds with Leu241, Arg243, Met240, and Asp447, with bond lengths of 2.87 Å, 3.10 Å, 3.04 Å, and 2.93 Å, respectively (Fig. 5B), and forms hydrophobic interaction with Arg364, Arg451, Ala280, Asp278, Phe436, Leu281 and Ser441. It can be speculated that the main interaction between LOX and RA is hydrogen bond and hydrophobic interaction.

4. Conclusion

The results showed that RA could effectively delay the lipid oxidation of fish meat, and US showed a synergistic effect. RA and US synergistically inhibited endogenous LOX related to lipid oxidation. The above results were confirmed by in vitro enzyme activity inhibition, multi spectroscopy and molecular docking experiments. This study provides a reference for the application of US and RA in the antioxidation and preservation of aquatic products, and also provides a basis for the basic mechanism of polyphenols inhibiting lipid oxidation in the process of food preservation.

CRediT authorship contribution statement

Ting-ting Chai: Conceptualization, Methodology, Formal analysis, Investigation, Data curation, Writing – original draft, Writing – review & editing, Visualization. **Yang-na Huang:** Methodology, Writing – review

& editing. **Shao-tian Ren:** Methodology, Writing – review & editing. **Dan-li Jin:** Methodology, Writing – review & editing. **Jing-jing Fu:** Methodology, Writing – review & editing. **Jun-yan Guo:** Validation, Investigation. **Yue-wen Chen:** Methodology, Resources, Supervision, Project administration, Funding acquisition.

Declaration of Competing Interest

The authors declare that they have no known competing financial interests or personal relationships that could have appeared to influence the work reported in this paper.

Acknowledgements

This work was financially supported by "National Key R&D Program of China (2018YFD0400600)", "Foundation of Zhejiang Educational Committee (Y201942135)" and "Zhejiang Provincial Natural Science Foundation (LQ21C200004)". The authors declare that there are no conflicts of interest.

References

[1] L. Jiao, C. Tu, J. Mao, S. Benjakul, B. Zhang, Impact of theaflavin soaking pretreatment on oxidative stabilities and physicochemical properties of semi-dried large yellow croaker (Pseudosciaena crocea) fillets during storage, Food Packag. Shelf Life 32 (2022), 100852.
[2] C. Bian, H. Cheng, H. Yu, J. Mei, J. Xie, Effect of multi-frequency ultrasound assisted thawing on the quality of large yellow croaker (Larimichthys crocea), Ultrason. Sonochem. 82 (2022), 105907.
[3] M. Utrera, D. Morcuende, R. Ganhão, M. Estévez, Role of phenolics extracting from Rosa canina L. on meat protein oxidation during frozen storage and beef patties processing, Food Bioproc. Technol. 8 (2014) 854–864.
[4] H. Du, C. Liu, O. Unsalan, C. Altunayar-Unsalan, S. Xiong, A. Manyande, H. Chen, Development and characterization of fish myofibrillar protein/chitosan/rosemary extract composite edible films and the improvement of lipid oxidation stability during the grass carp fillets storage, Int. J. Biol. Macromol. 184 (2021) 463–475.
[5] T. Li, W. Hu, J. Li, X. Zhang, J. Zhu, X. Li, Coating effects of tea polyphenol and rosemary extract combined with chitosan on the storage quality of large yellow croaker (Pseudosciaena crocea), Food Control 25 (2012) 101–106.
[6] D.C. Costa, H.S. Costa, T.G. Albuquerque, F. Ramos, M.C. Castilho, A. Sanches-Silva, Advances in phenolic compounds analysis of aromatic plants and their potential applications, Trends Food Sci. Technol. 45 (2015) 336–354.
[7] O. Fadel, K. El Kirat, S. Morandat, The natural antioxidant rosmarinic acid spontaneously penetrates membranes to inhibit lipid peroxidation in situ, Biochim. Biophys. Acta 1808 (2011) 2973–2980.
[8] N. Li, W. Liu, Y. Shen, J. Mei, J. Xie, Coating effects of ε-polylysine and rosmarinic acid combined with chitosan on the storage quality of fresh half-smooth tongue sole (Cynoglossus semilaevis Günther) fillets, Coatings 9 (2019) 273.
[9] F. Chemat, H. Zill, M.K. Khan, Applications of ultrasound in food technology: Processing, preservation and extraction, Ultrason. Sonochem. 18 (2011) 813–835.
[10] B. Liu, D.Y. Li, Z.X. Wu, W.J. Yang, D.Y. Zhou, B.W. Zhu, Combined effects of ultrasound and antioxidants on the quality maintenance of bay scallop (Argopecten irradians) adductor muscles during cold storage, Ultrason. Sonochem. 82 (2022), 105883.
[11] G. Huang, S. Chen, C. Dai, L. Sun, W. Sun, Y. Tang, F. Xiong, R. He, H. Ma, Effects of ultrasound on microbial growth and enzyme activity, Ultrason. Sonochem. 37 (2017) 144–149.
[12] T. Sae-leaw, S. Benjakul, K. Vongkamjan, Retardation of melanosis and quality loss of pre-cooked Pacific white shrimp using epigallocatechin gallate with the aid of ultrasound, Food Control 84 (2018) 75–82.
[13] Y.-W. Yuan, Y.-W. Chen, W.-Q. Cai, X.-P. Dong, Y.-R. Wang, L.-L. Zheng, Effects of sodium erythorbate and sodium tripolyphosphate on the lipid oxidation of Russian sturgeon with sous-vide cooking, J. Food Compos. Anal. 106 (2022), 104345.
[14] Y.-W. Chen, W.-Q. Cai, Y.-G. Shi, X.-P. Dong, F. Bai, S.-K. Shen, R. Jiao, X.-Y. Zhang, X. Zhu, Effects of different salt concentrations and vacuum packaging on the shelf-stability of Russian sturgeon (Acipenser gueldenstaedti) stored at 4 °C, Food Control 109 (2020), 106865.
[15] Q. Cao, Y. Huang, Q.F. Zhu, M. Song, S. Xiong, A. Manyande, H. Du, The mechanism of chlorogenic acid inhibits lipid oxidation: An investigation using multi-spectroscopic methods and molecular docking, Food Chem. 333 (2020), 127528.
[16] L. Sheng, P. Su, K. Han, J. Chen, A. Cao, Z. Zhang, Y. Jin, M. Ma, Synthesis and structural characterization of lysozyme–pullulan conjugates obtained by the Maillard reaction, Food Hydrocoll. 71 (2017) 1–7.
[17] J.-J. Fu, C. Sun, Z.-F. Tan, G.-Y. Zhang, G.-B. Chen, L. Song, Nanocomplexes of curcumin and glycated bovine serum albumin: The formation mechanism and effect of glycation on their physicochemical properties, Food Chem. 368 (2022), 130651.
[18] J. Zhu, X. Sun, S. Wang, Y. Xu, D. Wang, Formation of nanocomplexes comprising whey proteins and fucoxanthin: Characterization, spectroscopic analysis, and molecular docking, Food Hydrocoll. 63 (2017) 391–403.
[19] Z. Xu, Q. Cao, A. Manyande, S. Xiong, H. Du, Analysis of the binding selectivity and inhibiting mechanism of chlorogenic acid isomers and their interaction with grass carp endogenous lipase using multi-spectroscopic, inhibition kinetics and modeling methods, Food Chem. 382 (2022), 132106.
[20] C. Li, T. Dai, J. Chen, X. Li, T. Li, C. Liu, D.J. McClements, Protein-polyphenol functional ingredients: The foaming properties of lactoferrin are enhanced by forming complexes with procyanidin, Food Chem. 339 (2021), 128145.
[21] J. Jia, X. Gao, M. Hao, L. Tang, Comparison of binding interaction between beta-lactoglobulin and three common polyphenols using multi-spectroscopy and modeling methods, Food Chem. 228 (2017) 143–151.
[22] S.-K. Shen, Q.-Y. Bu, W.-T. Yu, Y.-W. Chen, F.-J. Liu, Z.-W. Ding, J.-L. Mao, Interaction and binding mechanism of lipid oxidation products to sturgeon myofibrillar protein in low temperature vacuum heating conditions: Multispectroscopic and molecular docking approaches, Food Chemistry: X 15 (2022), 100389.
[23] X. Tian, L. Rao, L. Zhao, Y. Wang, X. Liao, Multispectroscopic and computational simulation insights into the inhibition mechanism of epigallocatechin-3-gallate on polyphenol oxidase, Food Chem. 393 (2022), 133415.
[24] S. Jongberg, M.A. Torngren, A. Gunvig, L.H. Skibsted, M.N. Lund, Effect of green tea or rosemary extract on protein oxidation in Bologna type sausages prepared from oxidatively stressed pork, Meat Sci. 93 (2013) 538–546.
[25] Q. Cao, H. Du, Y. Huang, Y. Hu, J. You, R. Liu, S. Xiong, A. Manyande, The inhibitory effect of chlorogenic acid on lipid oxidation of grass carp (Ctenopharyngodon idellus) during chilled storage, Food Bioproc. Technol. 12 (2019) 2050–2061.
[26] S. Yamamoto, Mammalian lipoxygenases: molecular structures and functions, Biochim. Biophys. Acta (BBA) 1128 (1992) 117–132.
[27] L.M.G. Dalagnol, V.C.C. Silveira, H.B. da Silva, V. Manfroi, R.C. Rodrigues, Improvement of pectinase, xylanase and cellulase activities by ultrasound: Effects on enzymes and substrates, kinetics and thermodynamic parameters, Process Biochem. 61 (2017) 80–87.
[28] J. Chen, X. Zhang, X. Chen, A. Pius Bassey, G. Zhou, X., Xu, Phenolic modification of myofibrillar protein enhanced by ultrasound: The structure of phenol matters, Food Chem. 386 (2022), 132662.
[29] Q. Yu, L. Fan, Z. Duan, Five individual polyphenols as tyrosinase inhibitors: Inhibitory activity, synergistic effect, action mechanism, and molecular docking, Food Chem. 297 (2019), 124910.
[30] S. Banerjee, Inhibition of mackerel (Scomber scombrus) muscle lipoxygenase by green tea polyphenols, Food Res. Int. 39 (2006) 486–491.
[31] G. Jin, J. Zhang, X. Yu, Y. Lei, J. Wang, Crude lipoxygenase from pig muscle: partial characterization and interactions of temperature, NaCl and pH on its activity, Meat Sci. 87 (2011) 257–263.
[32] H. Su, Y.T. Ruan, Y. Li, J.G. Chen, Z.P. Yin, Q.F. Zhang, In vitro and in vivo inhibitory activity of taxifolin on three digestive enzymes, Int. J. Biol. Macromol. 150 (2020) 31–37.
[33] X. Zhao, J. Qi, C. Fan, B. Wang, C. Yang, D. Liu, Ultrasound treatment enhanced the ability of the porcine myofibrillar protein to bind furan compounds: Investigation of underlying mechanisms, Food Chem. 384 (2022), 132472.
[34] S. Bi, L. Yan, B. Pang, Y. Wang, Investigation of three flavonoids binding to bovine serum albumin using molecular fluorescence technique, J. Lumin. 132 (2012) 132–140.
[35] P. Han, N. An, L. Yang, X. Ren, S. Lu, H. Ji, Q. Wang, J. Dong, Molecular dynamics simulation of the interactions between sesamol and myosin combined with spectroscopy and molecular docking studies, Food Hydrocoll. 131 (2022), 107801.
[36] X. Peng, G. Zhang, Y. Liao, D. Gong, Inhibitory kinetics and mechanism of kaempferol on alpha-glucosidase, Food Chem. 190 (2016) 207–215.
[37] L. Shi, G. Xiong, T. Yin, A. Ding, X. Li, W. Wu, Y. Qiao, L. Liao, C. Jiao, L. Wang, Effects of ultra-high pressure treatment on the protein denaturation and water properties of red swamp crayfish (Procambarus clarkia), Lwt 133 (2020), 110124.
[38] Y. Cao, Y.L. Xiong, Chlorogenic acid-mediated gel formation of oxidatively stressed myofibrillar protein, Food Chem. 180 (2015) 235–243.
[39] H. Li, Y. Hu, X. Zhao, W. Wan, X. Du, B. Kong, X. Xia, Effects of different ultrasound powers on the structure and stability of protein from sea cucumber gonad, Lwt 137 (2021), 110403.
[40] Y. Li, Q.H. Zeng, G. Liu, Z. Peng, Y. Wang, Y. Zhu, H. Liu, Y. Zhao, J. Jing Wang, Effects of ultrasound-assisted basic electrolyzed water (BEW) extraction on structural and functional properties of Antarctic krill (Euphausia superba) proteins, Ultrason. Sonochem. 71 (2021), 105364.